# Two-dimensional exterior sound field reproduction using two rigid circular loudspeaker arrays



doi: 10.1121/10.0002280

# Two-dimensional exterior sound field reproduction using two rigid circular loudspeaker arrays

Yi Ren[1] and Yoichi Haneda[1]

*Graduate School of Informatics and Engineering, The University of Electro-Communications, Chofu, Tokyo 182-0026, Japan*[a)]

In exterior sound-field reproduction using loudspeaker arrays, such as a single circular array, there is a trade-off between the reproduction accuracy and the filter gain of the loudspeaker array. With the aim of reproducing complex sound fields with a lower filter gain, we introduce an asymmetrical array geometry with reflections between two or more rigid arrays. This paper proposes a sound field reproduction method using two rigid circular loudspeaker arrays in a circular harmonic domain. Transfer functions that consider the multiple scattering between two rigid baffles can be represented in the circular harmonic domain. By repeatedly transforming the expansion coefficient between two coordinate systems, the circular harmonic expansion was applied to the reproduced sound field in a mixed coordinate system. Then, the driving function of the loudspeaker arrays was derived through a mode expansion. Numerical simulations were conducted to verify the accuracy of the reproduced sound field.

 [http://dx.doi.org(DOI number)]

[XYZ] Pages: 1–11

## I. INTRODUCTION

Sound field reproduction using loudspeaker arrays has been studied for many years.[1] This technique reproduces the sound accurately over a space and allows every listener inside the space to perceive an immersive sound. Theoretically, a sound field can be synthesized by controlling the sound pressure and particle velocities on the boundary surface, based on the Kirchhoff–Helmholtz integral equation. This sound field reproduction technique is usually implemented with loudspeaker arrays by giving an individual signal to each loudspeaker. In recent decades, a variety of approaches have been proposed. Wave field synthesis is based on the Rayleigh integral and is the most common method for sound field reproduction.[2–5] Another well-known spatial-Fourier-transform-based method is called the mode-matching method,[6,7] the spectral division method,[8] or higher-order ambisonics.[9,10] Moreover, a pressure-matching method based on the simple source formulation[11] has been proposed.[12,13]

A circular loudspeaker array (CLA) is often used in sound field reproduction studies. Conventional systems that reproduce a sound field inside the CLA have a limited listening area,[14,15] which is determined by the size of the circular array. To achieve a boundless listening area, methods reproducing exterior sound fields using circular or spherical loudspeaker arrays have been proposed.[16,17]

With exterior sound-field reproduction systems, there is a trade-off between the reproduction accuracy and the filter gain, which is directly related to the output level of the loudspeakers. A high output level in a reproduction can cause nonlinear distortion and even physical damage to the loudspeaker. Therefore, a method to reproduce a sound field accurately with a sufficiently low filter gain is desired. For the CLA, there is a fixed mode strength (at each frequency), which relates the filter gain to the modes in the circular harmonic expansion. The more complex the desired field is, the more higher modes need to be used and the higher the filter gain will then be. Moreover, exterior sound-field-reproduction is often used for reproducing a specific radiation directivity or a focused source, which may have a relatively complex field. To reproduce such a complex field with a lower filter gain, we focus on the array geometry. That is, we consider that the array geometry limits the performance of a CLA. We suppose that it is possibly easier to reproduce such a sound field with a complex and irregular loudspeaker arrangement, including asymmetrical geometry and reflections.

A method using two circular loudspeaker arrays (2CLA) was proposed in our previous work.[18] In that study, we used two rigid CLAs, with an asymmetric geometry and multiple scattering between rigid baffles, to increase the complexity of the transfer function. A pressure-matching method based on multipoint sound-field control was then used for the sound field reproduction. As a result, the 2CLA was able to reproduce the sound field with higher accuracy, unlike a single CLA, for the same filter gain.

In this paper, we propose a method based on a circular harmonic expansion using the same array model. Instead of matching the sound pressure on the control points, this method matches the sound-field coefficient in the circular harmonic domain. Therefore, an analytic approach could be applied to reproduce the sound field,

[a)] ren.yi@uec.ac.jp

so that the influence of a discrete arrangement of sound sources and control points can be avoided.

In Sec. II, we describe the conventional mode-matching method based on a circular harmonic expansion. In Sec. III, we introduce the transfer function for the 2CLA derived in previous work,[18] with adjustments based on the multiple scattering theory.[19] Section IV introduces the proposed method, which is derived using Graf's addition theorem.[20] We developed a relationship between the modes of the loudspeaker arrays and the observation modes. Section V shows how the proposed method can easily be applied to multiple circular loudspeaker arrays (MCLA). In Sec. VI, we present the results of our numerical simulations. The necessity of considering the effect of multiple scattering is discussed first. Then we chose virtual source reproduction to test the reproduction accuracy. We examined the reproduction accuracy for single frequencies and compared the accuracy with that for the conventional CLA method[6] and the 2CLA method.[18] A simulation of a practical situation, in which the filter gain was constrained, was then conducted. Furthermore, we analyzed and discussed the mode strength of the 2CLA model.

## II. CIRCULAR HARMONIC EXPANSION

This section presents a spatial-Fourier-transform-based method for a CLA in conventional sound field reproduction studies. In this method, a two-dimensional sound field can be produced by reproducing the sound pressure on a continuous circular boundary of radius $r$.

The desired sound field $p(r,\phi,\omega)$ is first expanded using a circular harmonic expansion[11] with a basis of $e^{j\nu\phi}$:

$$p(r,\phi,\omega)=\sum_{\nu=-\infty}^{\infty}\mathring{p}_\nu(r,k)e^{j\nu\phi}, \tag{1}$$

where $\mathring{p}_\nu(r,k)$ is the coefficient of the $\nu$th mode. $\omega$ and $k$, which are the angular frequency and wavenumber, respectively, are partially omitted in this paper for simplicity. Note that only a two-dimensional sound field is discussed in this paper and $k=\omega/c$ for this condition. The sound field generated by continuous secondary sources on a circle can be expressed by

$$\hat{p}(r,\phi)=\int_0^{2\pi}G(r,\phi|r_0,\phi')d(\phi')r_0d\phi', \tag{2}$$

where $r_0$ is the radius of the circular source, and $G(r,\phi|r_0,\phi')$ and $d(\phi')$ are the transfer function and driving function, respectively. Applying a spatial Fourier transform to the right-hand side of (2) and using the orthogonality of the basis:

$$\int_0^{2\pi}e^{j\nu\phi}e^{-j\nu'\phi}d\phi=2\pi\delta_{\nu\nu'}, \tag{3}$$

where $\delta_{\nu\nu'}=1$ only if $\nu=\nu'$ and is, otherwise, 0. Thus, we obtain:

$$\hat{p}(r,\phi)=\sum_{\nu=-\infty}^{\infty}2\pi r_0\mathring{G}_\nu(r|r_0)\mathring{d}_\nu e^{j\nu\phi}, \tag{4}$$

where $\mathring{G}_\nu(r|r_0)$ and $\mathring{d}_\nu$ are the circular harmonic expansion coefficients of the transfer function $G(r,\phi|r_0,\phi')$ and the driving function $d(\phi')$, respectively.

To make the reproduced sound field the same as the original sound field, we can equate the circular harmonic expansion coefficients in (1) and (4). Thus, $\mathring{d}_\nu$ is derived as

$$\mathring{d}_\nu=\frac{\mathring{p}_\nu(r)}{2\pi r_0\mathring{G}_\nu(r|r_0)}. \tag{5}$$

This is the conventional method and is called the mode-matching method.[21] The driving function in the frequency domain can then be calculated using the inverse spatial Fourier transform:

$$d(\phi')=\sum_{\nu=-\infty}^{\infty}\mathring{d}_\nu e^{j\nu\phi'}. \tag{6}$$

The exterior sound field of a circular source can be reproduced using this method.

Furthermore, if we consider a CLA with discretely located loudspeakers, Eq. (2) can be rewritten as

$$\hat{p}(r,\phi)=\sum_{l=1}^{\mathcal{L}}G(r,\phi|r_0,\phi_l)d(\phi_l), \tag{7}$$

which implies that Eq. (5) can be written as

$$\mathring{d}_\nu=\frac{\mathring{p}_\nu(r)}{\mathcal{L}\mathring{G}_\nu(r|r_0)}. \tag{8}$$

Here, $\mathcal{L}$ denotes the number of loudspeakers.

## III. TRANSFER FUNCTION FOR TWO RIGID CIRCULAR ARRAYS

A model with parallel cylindrical rigid baffles has been discussed in conventional studies.[19] The scattering properties of this model have been explored not only in acoustics, but also in studies of electromagnetic waves. Most studies considered that the coordinate systems were at the center of each cylinder. In our previous work,[18] we used this approach to derive the transfer function of the 2CLA model.

We establish a reference coordinate system at the center of the sound field with origin $O$. For the 2CLA model, we have two other coordinate systems with origins at the center of the first array $O_1$ and at the center of the second array $O_2$. Thus, any point in the sound field can be represented by three sets of coordinates: $(r,\phi)$, $(r_1,\phi_1)$, and $(r_2,\phi_2)$. The configuration for 2CLA is shown in Fig. 1. The array index is $\zeta\in\{1,2\}$, the radius of array $\zeta$ is $r_{0,\zeta}$, and its center is at $(R_\zeta,\Phi_\zeta)$ in the reference coordinate system.

Unlike baffles with a simple shape, such as a cylinder or sphere, the wave will reflect between the baffles infinitely many times, which complicates the derivation of the transfer function for the two rigid circular arrays.

The sound field for the 2CLA can be expressed as the sum of the direct sound and reflections. Consider a single

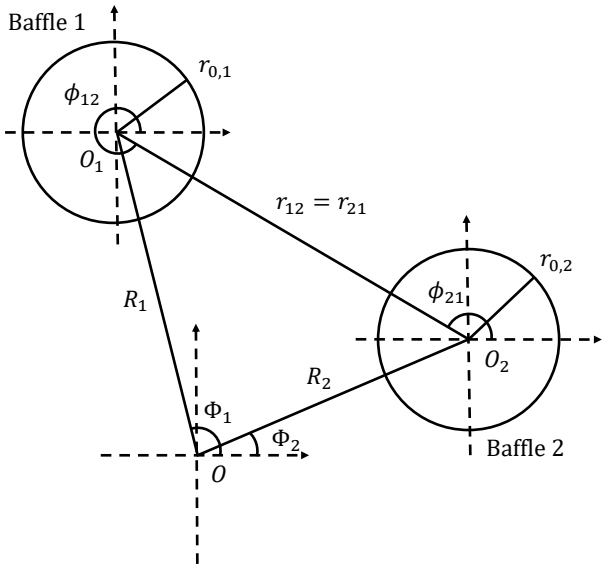


FIG. 1. Two rigid circles in a sound field.

reflection, in which a sound wave scattered by baffle 1 is incident on baffle 2. Graf's addition theorem[20] can be used for this transform. Therefore, any wave incident at baffle 2 that had been scattered by baffle 1 can be expressed as:

$$p_2^{\mathrm{i}}(r_2,\phi_2) = \sum_{\mu=-\infty}^{\infty}\sum_{\nu=-\infty}^{\infty} \gamma_{\nu,1} H_\nu(kr_1) e^{j\nu\phi_1} H_{\mu-\nu}(kr_{12}) e^{j(\mu-\nu)\phi_{12}} J_\mu(kr_2) e^{j\mu\phi_2}. \tag{9}$$

The opposite situation in which an incident wave at baffle 1 had been scattered by baffle 2 can be expressed as

$$p_1^{\mathrm{i}}(r_1,\phi_1) = \sum_{\mu=-\infty}^{\infty}\sum_{\nu=-\infty}^{\infty} \gamma_{\nu,2} H_\nu(kr_2) e^{j\nu\phi_2} H_{\mu-\nu}(kr_{21}) e^{j(\mu-\nu)\phi_{21}} J_\mu(kr_1) e^{j\mu\phi_1}. \tag{10}$$

where $(r_{12},\phi_{12})$ are the coordinates of the center of baffle 2 in coordinate system 1 and vice versa. Note that $r_{12} = r_{21}$ and $e^{j\phi_{12}} = -e^{j\phi_{21}}$ here. The time dependence in this study is given by $e^{j\omega t}$. $J_\nu(z)$ and $H_\nu(z)$ are the Bessel function of the first kind and the Hankel function of the second kind, respectively. The field incident at baffle 2 is reflected from its surface. The scattered sound can be derived with the Neumann boundary condition, which requires the particle velocity on the baffle to be 0 in the normal direction.[22] Thus, it is possible to calculate all the reflections between the two rigid baffles, and obviously, the transfer function is the sum of all these reflections.

Finally, we truncate the order of the circular harmonic expansion at $N$ as the error is sufficiently small. The transfer function of the 2CLA model can be expressed as a matrix product with the T matrix[19]:

$$G(r,\phi|r',\phi') = \boldsymbol{\psi}^{\mathrm{T}} \left( \sum_{i=0}^{\mathcal{R}} \mathbf{T}^i \right) \boldsymbol{\gamma}, \tag{11}$$

where $\mathcal{R}$ denotes the number of reflections and $\mathbf{T}^0 := \mathbf{I}$. We have:

$$\boldsymbol{\psi} = \left[ \boldsymbol{\psi}_1^{\mathrm{T}}, \boldsymbol{\psi}_2^{\mathrm{T}} \right]^{\mathrm{T}}, \tag{12}$$

$$\mathbf{T} = \begin{bmatrix} \mathbf{0}_{(2N+1)\times(2N+1)} & \mathbf{T}^{12} \\ \mathbf{T}^{21} & \mathbf{0}_{(2N+1)\times(2N+1)} \end{bmatrix}. \tag{13}$$

If the source is at baffle 1, then

$$\boldsymbol{\gamma} = [\boldsymbol{\gamma}_1^{\mathrm{T}}, \mathbf{0}_{1\times(2N+1)}]^{\mathrm{T}}, \tag{14}$$

and if the source is at baffle 2, then

$$\boldsymbol{\gamma} = [\mathbf{0}_{1\times(2N+1)}, \boldsymbol{\gamma}_2^{\mathrm{T}}]^{\mathrm{T}}. \tag{15}$$

With the index $\zeta \in \{1,2\}$, we have

$$\boldsymbol{\gamma}_\zeta = [\gamma_{-N,\zeta}(\mathbf{r}'_\zeta), \gamma_{-N+1,\zeta}(\mathbf{r}'_\zeta), \ldots, \gamma_{N,\zeta}(\mathbf{r}'_\zeta)]^{\mathrm{T}}, \tag{16}$$

$$\boldsymbol{\psi}_\zeta = [\psi_{-N,\zeta}(\mathbf{r}_\zeta), \psi_{-N+1,\zeta}(\mathbf{r}_\zeta), \ldots, \psi_{N,\zeta}(\mathbf{r}_\zeta)]^{\mathrm{T}}, \tag{17}$$

$$\mathbf{T}^{12} = \begin{bmatrix} T^{12}_{-N,-N} & T^{12}_{-N,-N+1} & \cdots & T^{12}_{-N,N} \\ T^{12}_{-N+1,-N} & T^{12}_{-N+1,-N+1} & \cdots & T^{12}_{-N+1,N} \\ \vdots & \vdots & \ddots & \vdots \\ T^{12}_{N,-N} & T^{12}_{N,-N+1} & \cdots & T^{12}_{N,N} \end{bmatrix}, \tag{18}$$

$$\mathbf{T}^{21} = \begin{bmatrix} T^{21}_{-N,-N} & T^{21}_{-N,-N+1} & \cdots & T^{21}_{-N,N} \\ T^{21}_{-N+1,-N} & T^{21}_{-N+1,-N+1} & \cdots & T^{21}_{-N+1,N} \\ \vdots & \vdots & \ddots & \vdots \\ T^{21}_{N,-N} & T^{21}_{N,-N+1} & \cdots & T^{21}_{N,N} \end{bmatrix}, \tag{19}$$

where

$$\gamma_{\nu,\zeta}(\mathbf{r}'_\zeta) = -\frac{e^{-j\nu\phi'_\zeta}}{2\pi k r_{0,\zeta} H'_\nu(kr_{0,\zeta})}, \tag{20}$$

$$\psi_{\nu,\zeta}(\mathbf{r}_\zeta) = H_\nu(kr_\zeta) e^{j\nu\phi_\zeta}, \tag{21}$$

$$T^{12}_{\nu,\mu} = -\frac{J'_\mu(kr_{0,2})}{H'_\mu(kr_{0,2})} H_{\nu-\mu}(kr_{12}) e^{j(\nu-\mu)\phi_{12}}, \tag{22}$$

$$T^{21}_{\nu,\mu} = -\frac{J'_\mu(kr_{0,1})}{H'_\mu(kr_{0,1})} H_{\nu-\mu}(kr_{21}) e^{j(\nu-\mu)\phi_{21}}. \tag{23}$$

Note that $r'_\zeta = r_{0,\zeta}$ if the source is at baffle $\zeta$. $J'_\nu(z)$ and $H'_\nu(z)$ are the differentials of the Bessel function of the first kind and the Hankel function of the second kind, respectively. Here, $\boldsymbol{\psi}$ and $\boldsymbol{\gamma}$ contain position information for the control points and loudspeakers, respectively, and $\mathbf{T}$ is a matrix that transforms a scattered sound into a reflected scattered sound. For computational convenience, the number of reflections is truncated to a finite number $\mathcal{R}$.

## IV. PROPOSED METHOD

In our previous study, a pressure-matching method was used with the 2CLA model for sound field reproduction.[18,23] Pressure matching is a simple method with a simple source formulation.[11] It can be applied to any array geometry with a known transfer function. On the other hand, this method needs to match the sound pressure at every control point on the boundary of the sound field and is a numerical approach.

To find a general solution of the 2CLA model, we first look for an analytic method. However, applying a mode-matching method to this model is difficult since the transfer functions of loudspeakers on different baffles are expressed in different coordinate systems. In recent years, studies of multizone sound reproduction and higher-order sources[24,25] have identified methods for controlling the sound in circular areas that are nonconcentric. There are two main aims for these methods:

- To expand the sound field using orthogonal bases, such as Bessel and Hankel functions.
- To describe the sound field in a reference coordinate system using Graf's addition theorem.

In this study, we aim to design a method that matches the sound-field coefficient by transforming the coordinate systems, while taking the multiple scattering effect (Sec. III) into account.

As in (2) and (6), the reproduced sound field of two discrete loudspeaker arrays (with $\mathcal{L}_\zeta$ loudspeakers, respectively) can be expressed as:

$$\hat{p}(r,\phi) = \sum_{l=1}^{\mathcal{L}_1} G(r,\phi|r_l,\phi_l) \sum_{\nu=-N_1}^{N_1} \mathring{d}_{\nu,1} e^{j\nu\phi_{l,1}} + \sum_{l'=1}^{\mathcal{L}_2} G(r,\phi|r_{l'},\phi_{l'}) \sum_{\nu'=-N_2}^{N_2} \mathring{d}_{\nu',2} e^{j\nu'\phi_{\nu',2}}, \tag{24}$$

where $G(r,\phi|r',\phi')$ is as in Sec. III. Here, $(r_l,\phi_l)$ is the position of the $l$th loudspeaker in the array. The truncation order for the circular harmonic expansion is set as $N_\zeta = \lfloor (L_\zeta - 1)/2 \rfloor$. Thanks to the orthogonality of $e^{j\nu\phi}$, (24) can be transformed to:

$$\hat{p}(r,\phi) = \boldsymbol{\psi}^{\mathrm{T}} \left( \sum_{i=0}^{\mathcal{R}} \mathbf{T}^i \right) \mathring{\boldsymbol{\Gamma}} \mathring{\mathbf{d}} \tag{25}$$

where

$$\mathring{\boldsymbol{\Gamma}} = \left[ \mathring{\boldsymbol{\Gamma}}_1^{\mathrm{T}}, \mathring{\boldsymbol{\Gamma}}_2^{\mathrm{T}} \right]^{\mathrm{T}}, \tag{26}$$

$$\mathring{\boldsymbol{\Gamma}}_\zeta = \mathcal{L}_\zeta \begin{bmatrix} \mathbf{0}_{(N-N_\zeta)\times(2N_\zeta+1)} \\ \mathrm{diag}(\mathring{\gamma}_{-N_\zeta,\zeta}, \mathring{\gamma}_{-N_\zeta+1,\zeta}, \ldots, \mathring{\gamma}_{N_\zeta,\zeta}) \\ \mathbf{0}_{(N-N_\zeta)\times(2N_\zeta+1)} \end{bmatrix}, \tag{27}$$

$$\mathring{\gamma}_{\nu,\zeta} = -\frac{1}{2\pi k r_{0,\zeta} H_\nu'(k r_{0,\zeta})}, \tag{28}$$

$$\mathring{\mathbf{d}} = \left[ \mathring{\mathbf{d}}_1^{\mathrm{T}}, \mathring{\mathbf{d}}_2^{\mathrm{T}} \right]^{\mathrm{T}}, \tag{29}$$

$$\mathring{\mathbf{d}}_\zeta = [\mathring{d}_{-N_\zeta,\zeta}, \mathring{d}_{-N_\zeta+1,\zeta}, \ldots, \mathring{d}_{N_\zeta,\zeta}]^{\mathrm{T}}. \tag{30}$$

To derive a relation between the driving functions of each mode and the sound-field coefficients in the circular harmonic domain, it is necessary to perform a coordinate transformation. $\mathring{d}_{\nu',2}$, expressed in the coordinate system at the origin $O_\zeta$ can be transformed to the coordinate system at $O$[26]:

$$\psi_{\nu,\zeta}(\mathbf{r}_\zeta) = \sum_{\nu'=-\infty}^{\infty} (-1)^{\nu-\nu'} J_{\nu-\nu'}(kR_\zeta) H_{\nu'}(kr) e^{j(\nu-\nu')\Phi_\zeta} e^{j\nu'\phi}. \tag{31}$$

Here, Graf's addition theorem[20] has been applied; therefore, the conditions $\nu'_{\max} \gg \nu$ and $r > R_\zeta$ must be satisfied. By truncating $\boldsymbol{\psi}$ in (25) for an sufficiently large $N$, it can be transformed to:

$$\boldsymbol{\psi} = \tilde{\mathbf{K}} \boldsymbol{\eta}, \tag{32}$$

where

$$\boldsymbol{\eta} = [\eta_{-N}(\mathbf{r}), \eta_{-N+1}(\mathbf{r}), \ldots, \eta_N(\mathbf{r})]^{\mathrm{T}}, \tag{33}$$

$$\eta_\nu(\mathbf{r}) = H_\nu(kr) e^{j\nu\phi}, \tag{34}$$

$$\tilde{\mathbf{K}} = \left[ \tilde{\mathbf{K}}_1^{\mathrm{T}}, \tilde{\mathbf{K}}_2^{\mathrm{T}} \right]^{\mathrm{T}}, \tag{35}$$

$$\tilde{\mathbf{K}}_\zeta = \begin{bmatrix} \tilde{\kappa}_{0,\zeta} & \tilde{\kappa}_{-1,\zeta} & \ldots & \tilde{\kappa}_{-2N,\zeta} \\ \tilde{\kappa}_{1,\zeta} & \tilde{\kappa}_{0,\zeta} & \ldots & \tilde{\kappa}_{-2N+1,\zeta} \\ \vdots & \vdots & \ddots & \vdots \\ \tilde{\kappa}_{2N,\zeta} & \tilde{\kappa}_{2N-1,\zeta} & \ldots & \tilde{\kappa}_{0,\zeta} \end{bmatrix}, \tag{36}$$

$$\tilde{\kappa}_{\nu,\zeta} = (-1)^\nu J_\nu(kR_\zeta) e^{j\nu\Phi_\zeta}. \tag{37}$$

Then the reproduced sound field can be transformed to

$$\hat{p}(r,\phi) = \boldsymbol{\eta}^{\mathrm{T}} \tilde{\mathbf{G}} \mathring{\mathbf{d}}, \tag{38}$$

where

$$\tilde{\mathbf{G}} = \tilde{\mathbf{K}}^{\mathrm{T}} \left( \sum_{i=0}^{\mathcal{R}} \mathbf{T}^i \right) \mathring{\mathbf{\Gamma}}. \tag{39}$$

The desired exterior sound field at the virtual observation points with a limited order $N$ can be expressed as

$$p(r,\phi) = \sum_{\nu=-N}^{N} \tilde{\alpha}_\nu H_\nu(kr) e^{j\nu\phi} \tag{40}$$

$$= \boldsymbol{\eta}^{\mathrm{T}} \tilde{\boldsymbol{\alpha}}, \tag{41}$$

where $\tilde{\alpha}_\nu$ is a sound-field coefficient[11]:

$$\tilde{\boldsymbol{\alpha}} = [\tilde{\alpha}_{-N}, \tilde{\alpha}_{-N+1}, \ldots, \tilde{\alpha}_N]^{\mathrm{T}}. \tag{42}$$

A relation between each mode of the loudspeaker arrays and the sound-field coefficient can be obtained from (39). Therefore, we can obtain the driving function in the circular harmonic domain. However, since this relation is not orthogonal, the driving function cannot be obtained directly. Therefore, the least-squares method with a Tikhonov regularization was applied as follows:

$$\mathring{\mathbf{d}} = \frac{\tilde{\mathbf{G}}^{\mathrm{H}} \tilde{\boldsymbol{\alpha}}}{\tilde{\mathbf{G}}^{\mathrm{H}} \tilde{\mathbf{G}} + \lambda \mathbf{I}}, \tag{43}$$

where $\lambda$ is a regularization parameter.

As in (6), the driving function for each loudspeaker can be obtained from

$$d_\zeta(\phi'_\zeta) = \sum_{\nu=-N_\zeta}^{N_\zeta} \mathring{d}_{\nu,\zeta} e^{j\nu\phi'_\zeta}. \tag{44}$$

## V. EXTENSION TO MULTIPLE CIRCULAR LOUDSPEAKER ARRAYS

In addition, the method proposed in this paper can be extended to MCLA. As in Sec. III, the transfer function of an MCLA with rigid baffles can be calculated with the T-matrix method.[19]

Consider an MCLA with $\mathcal{M}$ rigid circular arrays with array indexes $\mathcal{X}, \mathcal{Y} \in \{1, 2, \ldots, \mathcal{M}\}$ and $\mathcal{X} \neq \mathcal{Y}$. The T-matrix can be expressed as:

$$\mathbf{T} = \begin{bmatrix} \mathbf{0} & \mathbf{T}^{12} & \ldots & \mathbf{T}^{1\mathcal{M}} \\ \mathbf{T}^{21} & \mathbf{0} & \ldots & \mathbf{T}^{2\mathcal{M}} \\ \vdots & \vdots & \ddots & \vdots \\ \mathbf{T}^{\mathcal{M}1} & \mathbf{T}^{\mathcal{M}2} & \ldots & \mathbf{0} \end{bmatrix}, \tag{45}$$

$$\mathbf{T}^{\mathcal{XY}} = \begin{bmatrix} T^{\mathcal{XY}}_{-N,-N} & T^{\mathcal{XY}}_{-N,-N+1} & \cdots & T^{\mathcal{XY}}_{-N,N} \\ T^{\mathcal{XY}}_{-N+1,-N} & T^{\mathcal{XY}}_{-N+1,-N+1} & \cdots & T^{\mathcal{XY}}_{-N+1,N} \\ \vdots & \vdots & \ddots & \vdots \\ T^{\mathcal{XY}}_{N,-N} & T^{\mathcal{XY}}_{N,-N+1} & \cdots & T^{\mathcal{XY}}_{N,N} \end{bmatrix}, \tag{46}$$

$$T^{\mathcal{XY}}_{\nu,\mu} = -\frac{J'_\mu(kr_{0,\mathcal{Y}})}{H'_\mu(kr_{0,\mathcal{Y}})} H_{\nu-\mu}(kr_{\mathcal{XY}}) e^{j(\nu-\mu)\phi_{\mathcal{XY}}}. \tag{47}$$

The transfer function can be calculated in exactly the same as way (11), with the index extended to $\zeta \in \{1, 2, \ldots, \mathcal{M}\}$ and

$$\boldsymbol{\psi} = \left[ \boldsymbol{\psi}_1^{\mathrm{T}}, \boldsymbol{\psi}_2^{\mathrm{T}}, \ldots, \boldsymbol{\psi}_{\mathcal{M}}^{\mathrm{T}} \right]^{\mathrm{T}}, \tag{48}$$

$$\boldsymbol{\gamma} = [\mathbf{0}_{(\zeta-1)\times(2N+1)}, \boldsymbol{\gamma}_\zeta^{\mathrm{T}}, \mathbf{0}_{(\mathcal{M}-\zeta)\times(2N+1)}]^{\mathrm{T}}. \tag{49}$$

Since the transfer function is unchanged, the method proposed in Sec. IV applies to the MCLA. Thus, we can reproduce a sound field with MCLA with the same method as (43), where

$$\tilde{\mathbf{K}} = \left[ \tilde{\mathbf{K}}_1^{\mathrm{T}}, \tilde{\mathbf{K}}_2^{\mathrm{T}}, \ldots, \tilde{\mathbf{K}}_{\mathcal{M}}^{\mathrm{T}} \right]^{\mathrm{T}}, \tag{50}$$

$$\mathring{\mathbf{\Gamma}} = \left[ \mathring{\mathbf{\Gamma}}_1^{\mathrm{T}}, \mathring{\mathbf{\Gamma}}_2^{\mathrm{T}}, \ldots, \mathring{\mathbf{\Gamma}}_{\mathcal{M}}^{\mathrm{T}} \right]^{\mathrm{T}}, \tag{51}$$

$$\mathring{\mathbf{d}} = \left[ \mathring{\mathbf{d}}_1^{\mathrm{T}}, \mathring{\mathbf{d}}_2^{\mathrm{T}}, \ldots, \mathring{\mathbf{d}}_{\mathcal{M}}^{\mathrm{T}} \right]^{\mathrm{T}}. \tag{52}$$

Intrinsically, this method is similar to methods with higher-order sources[10,24,27] and higher-order microphones.[28–30] The difference in this paper is that the influence of the multiple scattering between the rigid baffles is taken into account.

## VI. NUMERICAL SIMULATIONS

In this section, we verify and evaluate the proposed method using numerical simulations of the reproduced sound field.

### A. Effects of multiple scattering

First, we verified the necessity of considering the effects of multiple scattering. Figure 2 shows the relative amplitude for each reflection for 2CLA, with arrays centered at $(-0.25\,\mathrm{m}, 0)$ and $(0.25\,\mathrm{m}, 0)$. The radii of both arrays are 0.15 m. The system is driven by a loudspeaker at $(-0.1\,\mathrm{m}, 0)$. In this type of setup, the reflections have a conspicuous effect. The relative amplitudes of the first and the second reflections are $-6.9\,\mathrm{dB}$ and $-13.5\,\mathrm{dB}$, respectively. Note that, conventionally, the sound field should be reproduced within an error of $-15\,\mathrm{dB}$ (about 4%). This indicates that it is necessary to take the effect of multiple scattering into account, especially for higher frequencies.

### B. Single frequency

To verify the performance in sound field reproduction, a numerical simulation of reproducing the sound

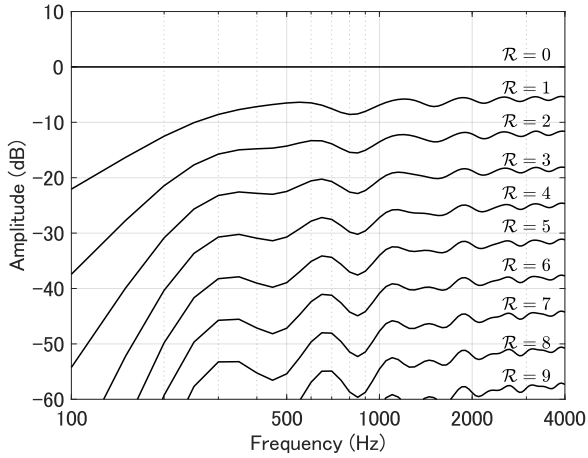


FIG. 2. Relative amplitude of each reflection of a 2CLA. The relative amplitude is evaluated from the sound pressure measured by a microphone at $(0, 2\,\mathrm{m})$. The amplitude of the direct sound ($\mathcal{R}=0$) is set to 0 dB as a reference. The truncation order is $N=30$.

field of a virtual sound source was conducted. In our proposed method, two loudspeaker arrays with 15 equally spaced loudspeakers were placed at $(-0.25\,\mathrm{m}, 0\,\mathrm{m})$ and $(0.25\,\mathrm{m},\ 0\,\mathrm{m})$, respectively. Both of these were rigid circular baffles with radii of 0.15 m. Up to 12 reflections were considered, and the maximum order was truncated at $N=30$ when calculating the transfer functions. The maximum order for the driving function was truncated to $N_1 = N_2 = \lfloor (15-1)/2 \rfloor = 7$. To avoid the singular matrix problem, the regularization parameter was set to $\lambda = \sigma_{\max}(\tilde{\mathbf{G}}^{\mathrm{H}}\tilde{\mathbf{G}}) \times 10^{-6}$ for the simulations above, where $\sigma_{\max}(\cdot)$ represents the maximum eigenvalue.

Figures 3 and 4 show the results. Figures 3(a) and 4(a) are the wavefronts of the desired sound fields and Figs. 3(d) and 4(d) are the wavefronts of the sound fields reproduced by the proposed method. White crosses mark the locations of the loudspeakers. The target virtual sound source was an omnidirectional line source at 1000 Hz, which was at $(0\,\mathrm{m},\ 0.5\,\mathrm{m})$ for Fig. 3 and at $(0.5\,\mathrm{m},\ 0\,\mathrm{m})$ for Fig. 4. Since the array geometry is asymmetric, using two virtual sources here also aims to verify the asymmetry in the results.

The results of the conventional methods are also shown. Figures 3(b) and 4(b) are for a CLA with a radius of 0.15 m and 30 loudspeakers, using the mode-matching method. The maximum order of the driving function was truncated to $\lfloor (30-1)/2 \rfloor = 14$. Figures 3(c) and 4(c) are for the same 2CLA using the pressure-matching method with 144 microphones on a 2-m-radius circle. The regularization parameter was set to $\sigma_{\max}(\mathbf{G}^{\mathrm{H}}\mathbf{G}) \times 10^{-6}$, where $\mathbf{G}$ is the transfer function matrix.

The reproduction errors of each method are shown in Figs. 3(e)–3(g) and 4(e)–4(g), with respect to Figs. 3(b)–3(d) and 4(b)–4(d). The errors were calculated using:

$$\varepsilon(\mathbf{x}) = 10\log_{10}\frac{|p(\mathbf{x})-\hat{p}(\mathbf{x})|^2}{|p(\mathbf{x})|^2}. \tag{53}$$

The maximum filter gains in Figs. 3(b)–3(d) and 4(b)–4(d) were 105.6, 23.1, 23.0, 107.7, 9.2, and 9.2 dB, respectively. This maximum filter gain was evaluated using the maximum amplitude of the driving function for all loudspeakers:

$$g = 10\log_{10}\frac{\max|d_{\zeta}(\phi'_{\theta})|^2}{|A_0|^2}. \tag{54}$$

where $A_0$ is the amplitude of the target virtual source.

Comparing the wavefronts and errors in Figs. 3 and 4, we can see that the proposed method and conventional methods all reproduced the sound field with an ideal accuracy. This indicates that the proposed method is valid for sound field reproduction. The results for the pressure-matching method and mode-matching method are similar, although the proposed mode-matching method has the advantage of being able to analyze and truncate by the orders. The CLA with the conventional method had the smallest error. However, the filter gain of CLA was much higher than that of 2CLA, which will result in a high output level.

Next, to investigate the reproduction of a complex field, we conducted a simulation with six random target virtual sources. All the virtual sources had amplitudes randomized between 0 and 1, phases randomized between 0 and $2\pi$, positions randomized inside a circle with a radius of 0.5 m, and randomized directivities. Each directivity was synthesized by a combination of a monopole and a dipole, in a random direction and with a random weight. The array configuration and other conditions were the same as above. The pressure-matching method was not included in this part.

Figure 5(a)–5(c) are the wavefront of the desired sound field, the reproduced sound field of CLA, and the reproduced sound field of 2CLA, respectively. Figure 5(d) and 5(e) show the reproduction error of CLA and 2CLA. We evaluted the spatial average error in an area $\Omega$, which is the ring area between radii of 1 m and 4 m:

$$\varepsilon_{\Omega} = 10\log_{10}\frac{\int_{\Omega}|p(\mathbf{x})-\hat{p}(\mathbf{x})|^2 d\mathbf{x}}{\int_{\Omega}|p(\mathbf{x})|^2 d\mathbf{x}}. \tag{55}$$

The errors of CLA and 2CLA were -54.4 and -37.7 dB, respectively. The filter gains of CLA and 2CLA were 101.1 and 5.6 dB, respectively. Furthermore, 1000 trails were taken on randomly generated sources, the average error of CLA and 2CLA were -50.0 and -20.2 dB where the average filter gains of CLA and 2CLA were 106.8 and 19.6 dB. From the above, we can know that both arrays had acceptable reproduction errors while CLA had significantly higher filter gains than 2CLA.

### C. Narrowband

We also conducted another simulation with a narrowband signal to investigate the relation between the filter

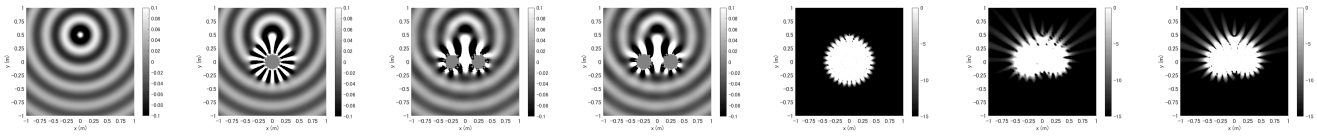

(a) (b) (c) (d) (e) (f) (g)

FIG. 3. Comparison of the desired sound field and the reproduced sound field, with a 1000 Hz omnidirectional virtual source at (0 m, 0.5 m). (a) The desired sound field. (b) Sound field reproduced by a CLA. (c) Sound field from our previous study reproduced by a 2CLA using the pressure-matching method.[18] (d) Sound field reproduced by a 2CLA using the proposed method. (e)–(g) Reproduction error (in dB) of (b)–(d), respectively.

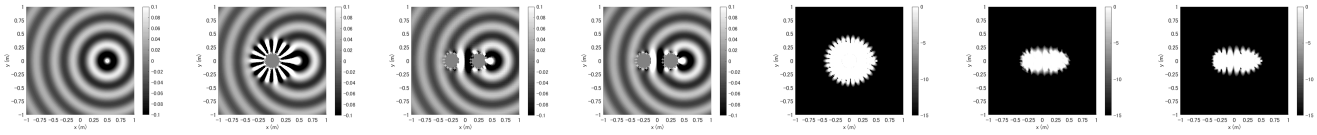

(a) (b) (c) (d) (e) (f) (g)

FIG. 4. Comparison of the desired sound field and the reproduced sound field, with a 1000 Hz omnidirectional virtual source at (0.5 m, 0 m). (a) The desired sound field. (b) Sound field reproduced by a CLA. (c) Sound field from our previous study reproduced by a 2CLA using the pressure-matching method.[18] (d) Sound field reproduced by a 2CLA using the proposed method. (e)–(g) Reproduction error (in dB) of (b)–(d), respectively.

gain and the performance. We used the frequency band 200–1500 Hz and compared the proposed method with 2CLA to that with CLA. The arrays used in this simulation were the same as those used for Figs. 3 and 4. The original field was also produced with an omnidirectional virtual source at (0 m, 0.5 m) or (0.5 m, 0 m). For the CLA, the results do not vary by direction because of the symmetric geometry. Here, we show only the result for the virtual source at (0 m, 0.5 m) for CLA. For the 2CLA, $\varphi$ is the direction of the virtual source. Thus, $\varphi = 0°$ and $\varphi = 90°$ are for the virtual source at (0.5 m, 0 m) and (0 m, 0.5 m), respectively. Figure 6 shows the maximum filter gain and the error of the proposed method for the CLA. The filter gain was calculated by (54). and the error was evaluated by (55) in the ring area between radii of 1 m and 4 m.

In this paper, as noted in Sec. VI A, we consider −15 dB as a threshold for the reproduction error. For frequencies over 1500 Hz, none of these methods could reproduce the sound field well. Therefore, higher frequencies are not discussed in this paper. Although CLA had the best accuracy (with a reproduction error of less than −50 dB), the filter gain was more than 100 dB higher than 2CLA at lower frequencies. Moreover, 2CLA gave acceptable results. It had a reproduction error of less than −15 dB for $\varphi = 0°$ and a relatively low filter gain. Note that it is also a disadvantage of 2CLA once higher accuracy is needed. On the other hand, we found that the results for 2CLA vary with direction, and $\varphi = 0°$ performed best here. One can infer that 2CLA achieved lower filter gain at the expense of the accuracy. Considering a trade-off between the reproduction accuracy and the filter gain may exist, we had a further comparison at a certain filter gain in Sec. VI D.

### D. Constrained filter gain

To evaluate the proposed method in a practical situation in which the loudspeakers have a lower output level, we conducted a numerical simulation of a filter gain controlling method. For a least-squares method with Tikhonov regularization, it is possible to constrain the L2-norm with the regularization parameter.[31] Besides, the L2-norm in (43), $||\mathring{\mathbf{d}}||^2$, is related to the filter gain. Therefore, we used the regularization parameter $\lambda$ in (43) to constrain the filter gain to 0 dB. We compared the results for CLA and 2CLA. The simulation conditions were similar to those used for Fig. 6. The only difference was that we tested four values of $\varphi$ (the direction of the virtual source) for 2CLA to see how $\varphi$ is related to the performance. As shown in Fig. 7, 2CLA performs better than CLA for the same filter gain. This means that the 2CLA model can reproduce a sound field more easily than CLA with a higher radiation efficiency. Moreover, the results indicate that there is a relation between the performance of 2CLA and the direction of the virtual source, since 2CLA performs better for smaller $\varphi$ ($\varphi \in [0°, 90°]$ because of reflectional symmetry).

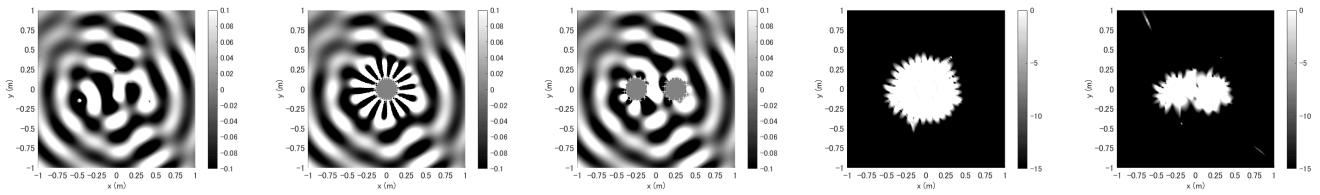

(a) (b) (c) (d) (e)

FIG. 5. Results on reproducing a complex field with six random target virtual sources. (a) The desired sound field. (b) Sound field reproduced by a CLA. (c) Sound field reproduced by a 2CLA. (d) and (e) Reproduction error (in dB) of (b) and (c), respectively.

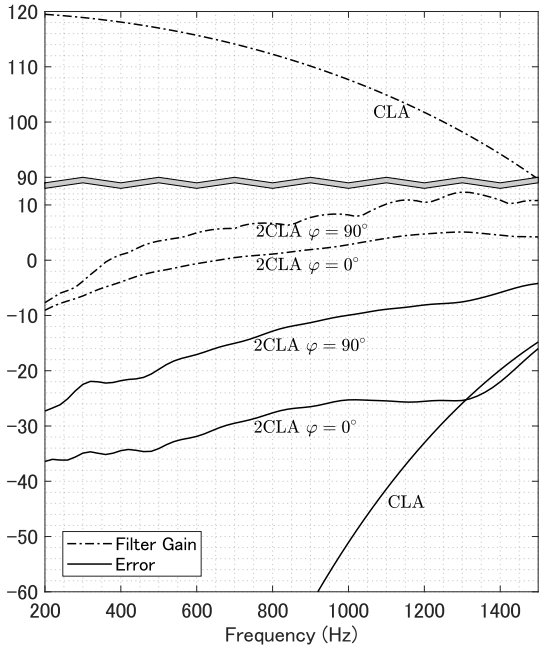


FIG. 6. Filter gain and normalized reproduction error (in dB) for 2CLA and CLA using the mode-matching method. Note the break in the $y$-axis between 15 and 90 dB.

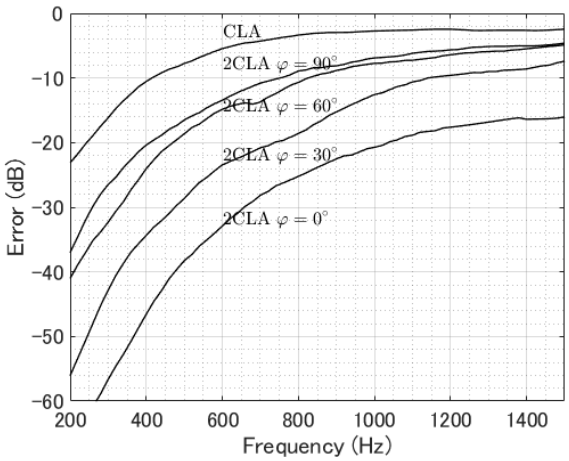


FIG. 7. Normalized reproduction error of 2CLA and CLA with a filter gain of 0 dB.

### E. Temporal response

We also checked the temporal response at listening positions to assess whether there are any temporal errors caused by the reflections between the two rigid arrays. A monopole virtual source was set at (0 m, 0.5 m). The target signal was a pulse (the amplitude at the source location was 1) and we applied a band-pass filter to the signal, ranged from 200–1500 Hz. The other simulation conditions were the same as in Sec. VI D. The filter gain was constrained to 0 dB. Figure 8 shows the results at the listening position (0 m, 1.5 m), which is in front of the target source. The reproduced signal matched the impulse response of the target source at the listening position. This indicates that the multiple scattering between the arrays has little negative effect on the reproduction.

### F. Three-dimensional time-domain simulation

To explore the suitability of the proposed method with rigid cylindrical arrays, we conducted time-domain simulations in a three-dimensional field. A finite-difference time-domain[32] method was used for the simulations. We conducted two simulations at 500 and 1000 Hz. Sinusoidal waves were used as the source signal. We applied the filter gain suppression method of Sec. VI D. According to the results in Fig. 7, a virtual source at (0 m, 0.5 m) and at a frequency under 500 Hz can be reproduced in ideal conditions. We, therefore, set a virtual source at (0 m, 0.5 m) for simulation at 500 Hz and a virtual source at (0 m, 0.3 m), which is easier to reproduce, for simulation at 1000 Hz. We used the same 2CLA model as in the previous simulations except that

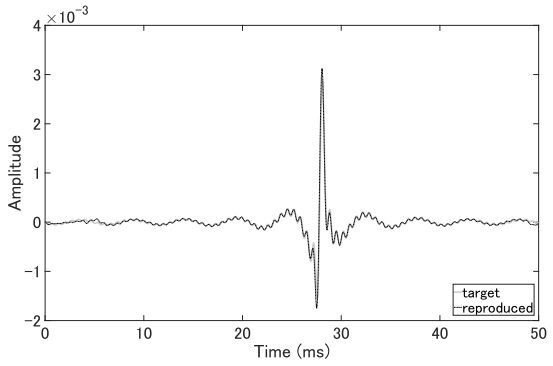


FIG. 8. Temporal response at listening position (0 m, 1.5 m). The gray line is the target signal and the black line is the reproduced signal.

the rigid circular baffles were two rigid cylindrical baffles with a finite height of 0.576 m. The loudspeakers were modeled as point sources on a horizontal surface in the three-dimensional field. We set the size of the space grid to 0.01 m for all axes and the time step to $1.0 \times 10^{-5}$ s. A method based on perfectly matched layers[33] was used to avoid redundant reflections from boundaries.

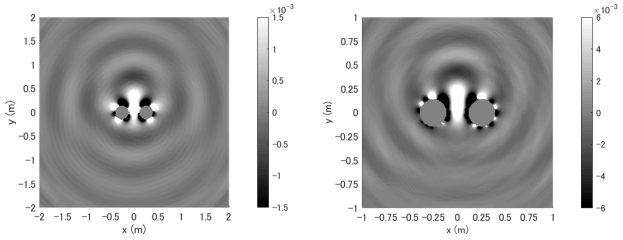


(a) (b)

FIG. 9. Wavefronts in the horizontal surface of the reproduced sound field in the three-dimensional time-domain simulation: (a) 500 Hz target source at (0 m, 0.5 m) and (b) 1000 Hz target source at (0 m, 0.3 m).

Figure 9 shows the wavefronts in the horizontal surface of the reproduced sound field. Note that we show a $2 \times 2\,\mathrm{m}^2$ area in Fig. 9(a) for clarity. In this simulation, the conditions were mismatched. The filter were obtained in the two-dimensional assumption while the simulation was conducted in a three-dimensional sound field with a finite-height cylinder. Therefore, an exactly matched results can not be expected. However, the results show that there was no significant deformation of the wavefronts and the reproduced sound field was similar to the desired sound field. This indicates that the proposed method is, to some extent, suitable for cylindrical arrays.

### G. Mode strength

The numerical simulations of Secs. VI B to VI D indicate that 2CLA can reproduce virtual sources more easily than CLA. Here, we investigate the general properties of 2CLA. In (43) for the transfer function in the circular harmonic domain, $\tilde{\mathbf{G}}$ is the primary factor affecting the difficulty in achieving a reproduction. Here, we focus on the power of $\tilde{\mathbf{G}}$, which represents the mode strength in CLA, to see how the array geometry actually affects the sound field reproduction.

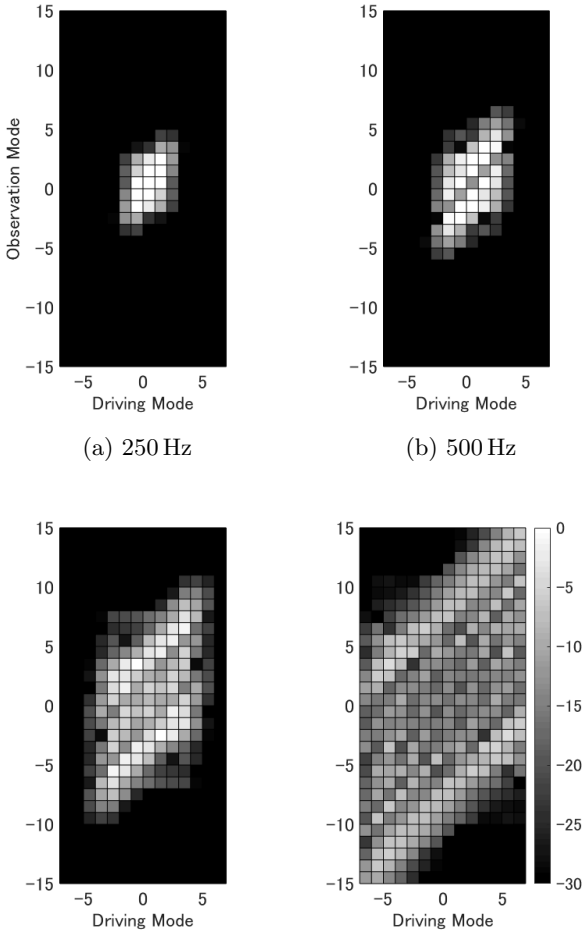


(a) 250 Hz (b) 500 Hz

(c) 1000 Hz (d) 2000 Hz

FIG. 10. Power of $\tilde{\mathbf{G}}$ (in dB).

The power of $\tilde{\mathbf{G}}$ is shown in Fig. 10. The $x$-axis represents the driving modes of 2CLA and the $y$-axis represents the observation modes for the secondary sound field. A driving mode is the mode used for driving loudspeakers, whereas an observation mode is the mode observed on the circle centered at the origin $O$. The results show how an observation mode can be synthesized from the driving modes. A high mode strength indicates that the driving mode can easily be used to synthesize the observation mode.

We found that driving a single mode of the 2CLA generates multiple modes in the field. On the other hand, each mode of a CLA is usually related to only one observation mode. Thus, we obtained two properties of 2CLA:

1. The lower modes of a driving function can be used to synthesize higher modes in the field. This indicates that 2CLA has good potential for reproducing complex fields.

2. Conversely, higher driving modes are needed in synthesizing lower modes. If only lower modes are used, there will be errors and the amplitudes will depend on the frequency. Therefore, 2CLA can be less useful for reproducing simple fields.

## VII. CONCLUSION

In this paper, we proposed an exterior sound-field reproduction method using 2CLA with rigid baffles in a circular harmonic domain. To obtain an analytic reproduction method, we used a harmonic circular expansion to remove the influence of the discrete arrangement of sound sources and control points. We derived the relation between each mode of the loudspeaker arrays and the sound-field coefficient of the reproduced sound field by applying a coordinate transformation. Computer simulations were conducted and the results show that the proposed method can reproduce the sound field. Moreover, the mode strength of 2CLA was discussed. It was inferred that 2CLA has good potential for reproducing complex fields. In addition, this method can be easily extended to multiple circular arrays.

## ACKNOWLEDGMENTS

This research was supported by JSPS KAKENHI Grant Number 19K12041.

[1]J. Ahrens, *Analytic Methods of Sound Field Synthesis* (Springer Science & Business Media, 2012).

[2]A. J. Berkhout, D. de Vries, and P. Vogel, "Acoustic control by wave field synthesis," J. Acoust. Soc. Am. **93**(5), 2764–2778 (1993).

[3]M. M. Boone, E. N. Verheijen, and P. F. Van Tol, "Spatial sound-field reproduction by wave-field synthesis," J. Audio Eng. Soc. **43**(12), 1003–1012 (1995).

[4]W. P. J. De Bruijn, "Application of wave field synthesis in videoconferencing," Ph.D. thesis, Delft University of Technology, 2004.

[5]S. Spors, R. Rabenstein, and J. Ahrens, "The theory of wave field synthesis revisited," in *Proceedings of the 124th Convention of the AES* (2008).

[6]M. A. Poletti, "A unified theory of horizontal holographic sound systems," J. Audio Eng. Soc. **48**(12), 1155–1182 (2000).

[7]M. A. Poletti, "Three-dimensional surround sound systems based on spherical harmonics," J. Audio Eng. Soc. **53**(11), 1004–1025 (2005).

[8]J. Ahrens and S. Spors, "Analytical driving functions for higher order ambisonics," in *Proceedings of the IEEE International Conference on Acoustics, Speech and Signal Processing (ICASSP)* (2008), pp. 373–376.

[9]J. Daniel, "Spatial sound encoding including near field effect: Introducing distance coding filters and a viable, new ambisonic format," in *Proceedings of the 23rd International Conference of the AES: Signal Processing in Audio Recording and Reproduction* (2003).

[10]A. Gupta and T. D. Abhayapala, "Three-dimensional sound field reproduction using multiple circular loudspeaker arrays," IEEE Trans. Audio Speech Lang. Proc. **19**(5), 1149–1159 (2011).

[11]E. G. Williams, *Fourier Acoustics: Sound Radiation and Nearfield Acoustical Holography* (Elsevier, 1999).

[12]O. Kirkeby and P. A. Nelson, "Reproduction of plane wave sound fields," J. Acoust. Soc. Am. **94**(5), 2992–3000 (1993).

[13]M. Kolundzija, C. Faller, and M. Vetterli, "Reproducing sound fields using MIMO acoustic channel inversion," J. Audio Eng. Soc. **59**, 721–734 (2011).

[14]J. Hannemann and K. D. Donohue, "Virtual sound source rendering using a multipole-expansion and method-of-moments approach," J. Audio Eng. Soc. **56**(6), 473–481 (2008).

[15]R. G. Oldfield, "The analysis and improvement of focused source reproduction with wave field synthesis," Ph.D. thesis, University of Salford, 2013.

[16]I.-Y. Jeon and J.-G. Ih, "On the holographic reconstruction of vibroacoustic fields using equivalent sources and inverse boundary element method," J. Acoust. Soc. Am. **118**(6), 3473–3482 (2005).

[17]W.-H. Cho, "Sound source modelling and synthesis by the equivalent source method for reproducing the spatial radiation characteristics," in *Proceedings of the 2016 International Conference of the AES: Sound Field Control* (2016).

[18]Y. Ren and Y. Haneda, "Virtual source reproduction using two rigid circular loudspeaker arrays," in *Proceedings of the 145th Conference of the AES* (2018).

[19]P. A. Martin, *Multiple Scattering: Interaction of Time-harmonic Waves with N Obstacles*, Encyclopedia of Mathematics and its Applications, No. 107 (Cambridge University Press, 2006).

[20]G. N. Watson, *A Treatise on the Theory of Bessel Functions* (Cambridge University Press, 1995).

[21]F. M. Fazi, M. Shin, F. Olivieri, S. Fontana, and Y. Lang, "Comparison of pressure-matching and mode-matching beamforming for methods for circular loudspeaker arrays," in *Proceedings of the 137th Convention of the AES* (2014).

[22]S. Koyama, K. Furuya, Y. Hiwasaki, Y. Haneda, and Y. Suzuki, "Sound field reproduction using multiple linear arrays based on wave field reconstruction filtering in helicalwave spectrum domain," in *Proceedings of the IEEE International Conference on Acoustics, Speech and Signal Processing (ICASSP)* (2013), pp. 271–275.

[23]Y. Ren and Y. Haneda, "How the distance and radius of two circular loudspeaker arrays affect sound field reproduction and directivity controls," in *Proceedings of the 23rd International Congress on Acoustics* (2019).

[24]M. A. Poletti, T. D. Abhayapala, and P. Samarasinghe, "Interior and exterior sound field control using two dimensional higher-order variable-directivity sources," J. Acoust. Soc. Am. **131**(5), 3814–3823 (2012).

[25]M. A. Poletti, T. Betlehem, and T. D. Abhayapala, "Comparison of sound reproduction using higher order loudspeakers and equivalent line arrays in free-field conditions," J. Acoust. Soc. Am. **136**(1), 192–200 (2014).

[26]Y. J. Wu and T. D. Abhayapala, "Spatial multizone soundfield reproduction: Theory and design," IEEE Trans. Audio Speech Lang. Proc. **19**(6), 1711–1720 (2011).

[27]M. A. Poletti and T. D. Abhayapala, "Spatial sound reproduction systems using higher order loudspeakers," in *Proceedings of the IEEE International Conference on Acoustics, Speech and Signal Processing (ICASSP)* (2011), pp. 57–60.

[28]T. D. Abhayapala and A. Gupta, "Spherical harmonic analysis of wavefields using multiple circular sensor arrays," IEEE Trans. Audio Speech Lang. Proc. **18**(6), 1655–1666 (2010).

[29]P. Samarasinghe, T. Abhayapala, and M. Poletti, "Wavefield analysis over large areas using distributed higher order micro-

phones," IEEE/ACM Trans. Audio Speech Lang. Proc. **22**(3), 647–658 (2014).

[30]N. Ueno, S. Koyama, and H. Saruwatari, "Sound field recording using distributed microphones based on harmonic analysis of infinite order," IEEE Signal Proc. Lett. **25**(1), 135–139 (2017).

[31]H. L. Van Trees, *Optimum Array Processing: Part IV of Detection, Estimation, and Modulation Theory* (John Wiley & Sons, 2004).

[32]K. Yee, "Numerical solution of initial boundary value problems involving maxwell's equations in isotropic media," IEEE Trans. Ant. Prop. **14**(3), 302–307 (1966).

[33]J. Berenger, "A perfectly matched layer for the absorption of electromagnetic waves," J. Comput. Phys. **114**(2), 185–200.